Intrinsic Euler-Lagrange Dynamics and Control Analysis of the Ballbot

Aykut C. Satici, Fabio Ruggiero, Vincenzo Lippiello and Bruno Siciliano

Abstract— **Research on bipedal locomotion has shown that a dynamic walking gait is energetically more efficient than a statically stable one. Analogously, even though statically stable multi-wheeled robots are easier to control, they are energetically less efficient and have low accelerations to avoid tipping over. In contrast, the ballbot is an underactuated, nonholonomically constrained mobile robot, upward equilibrium point of whose body has to stabilized by active controls. In this work, we derive coordinate-invariant equations of motion for the ballbot. We present the linearized equations of motion followed by its controllability analysis. Excluding the rotary degree of freedom of the ball in the inertial vertical direction, the linear system turns out to be controllable. It follows that the nonlinear system is locally controllable and we provide a proportional-derivative type controller that locally exponentially stabilizes the upward equilibrium point as well as the translation of the ball. The basin of attraction turns out to be large in the simulation studies.**

I. Introduction

Contemporary research on robotics has steered towards the incorporation of robots into everyday lives of humans. Robots are expected to safely interact with humans both outdoors and in human environments. This motivation requires robots not only to be mobile and slim but also tall enough to facilitate interaction. On the other hand, conventional multi-wheeled statically-stable robots are typically built to have a low center of gravity in order to prevent them from easily tipping over. The satisfaction of these two conflicting requirements urges the mobile robots to have large, wide, and heavy bases. At the cost of the necessity to design a more complicated controller, a more efficient method to tackle the interaction problem is to utilize dynamically stable robots.

One of the most popular dynamically balancing robots is the two-wheeled Segway [1]. The ballbot was introduced as a mobile robot moving on a single spherical omnidirectional wheel [2], [3]. It is typically slim and as tall as an adult human, rendering it able to interact with humans while navigating constrained environments [4], [5].

Even though a variant of this robot has been built by many laboratories [6], [7], its control framework has been restricted to the use of classic methods such as linearization in coordinates and PID controllers [7], [8]. Moreover, many controllers are typically developed by restricting the dynamics of the ballbot to a vertical 2D plane and applied to the 3D robot by an *ad-hoc* extension to two distinct vertical planes. This procedure inevitably ignores the energetic interaction of the full dynamics of the robot along these planes. Trajectory planning based on motion primitives has been presented in [9], while in [10], authors plan a trajectory for the ballbot equipped with right and left arms. A sliding-mode controller has also been designed for this system in [11]. For the most part, the equations of motion of the full dynamics of the ballbot have been derived in coordinates, which injects a fair bit of unnecessary complexity into the problem formulation, requires the use of a symbolic manipulation software and a decent amount of storage space in the computer [7]. The only exception to this trend has been provided in [12], where the authors derive a dynamic model of the ballbot which additionally assumes that the body has no yaw motion relative to the ball using Newton's laws. This lengthy procedure, which was omitted from the paper due to space considerations, leads to a dynamical model of the system which is not particularly easy to work with for control synthesis.

In this paper, we derive the Euler-Lagrange equations of motion of the full dynamics of the ballbot without resort to any coordinate system. This yields a compact, yet explicit representation of the equations of motion, which recover the 2D dynamics of the ballbot, restricted to a vertical plane, given in the literature [5]. Taking the variation of the equations of motion, we derive the linearized dynamics whose controllability analysis is then performed. This analysis reveals that controllable subsystem consists of all directions but the rotation of the ball along the inertial vertical direction. According to conventional linear control theory, a state-feedback control law exists that exponentially stabilizes the origin of the controllable subsystem of the linear system. Identifying this linear control law as the variation of a certain nonlinear control law, we are able to locally exponentially stabilize the upward equilibrium point of the ballbot as well as the translation of the ball to any desired point. The development of the controller through the coordinate-invariant linearization allows us to avoid representation singularities which typically plague similar controllers relying on coordinates. Simulation studies indicate that the basin of attraction of this controller is reasonably large. The main contribution of this paper is providing an intrinsic and unified framework to study the dynamics and control of the balancing system consisting of a heavy top on a spherical wheel.

II. Lagrangian Dynamics of the Ballbot

In this section, we present the background information to be used in the remainder of this paper including the kinematics

The research leading to these results has been supported by the RoDyMan project, which has received funding from the European Research Council FP7 Ideas under Advanced Grant agreement number 320992. The authors are solely responsible for the content of this manuscript.

A.C. Satici, F. Ruggiero, V. Lippiello and B. Siciliano are with the PRISMA Lab and CREATE Consortium, Dipartimento di Ingegneria Elettrica e Tecnologie dellInformazione, Università degli Studi di Napoli Federico II, via Claudio 21, 80125, Naples, Italy. Corresponding author: Aykut C. Satici - acsatici@utdallas.edu.

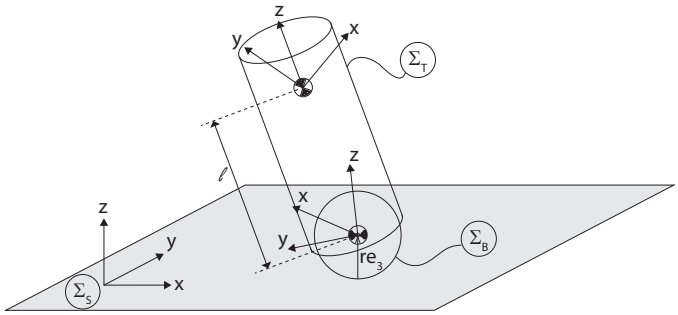

Fig. 1: Ballbot: bodies and frames

and dynamics of the ballbot. Note that, every vector quantity in this paper is represented in the spatial frame.

A. Background and Kinematics

The skeleton diagram of the ballbot is depicted in Figure 1. It is constructed by connecting a rigid spherical wheel to a rigid cylindrical body such that the body is unable to translate with respect to the ball but is free to move otherwise. Therefore, the configuration manifold of the ballbot is $Q = \mathbb{R}^2 \times SO(3) \times SO(3)$. The inertial frame, denoted by Σ_S, is fixed to a horizontal plane. The spherical wheel is represented by the frame Σ_B and is assumed to have its center of mass at its geometric center. As a result, the vector from the point of contact of the sphere with the ground and its center of mass is given by re_3 in the inertial frame. Here, r denotes the radius of the sphere and throughout the paper e_n denotes the n^{th} standard unit vector. The cylindrical rigid body situated on the wheel is referred to as the "top" and is bestown a reference frame denoted by Σ_T. The center of mass of the top is assumed to lie on the central axis of its geometrical shape at a distance $l > 0$ from the center of the ball. The ball is assumed to roll without slipping, yielding the well-known nonholonomic constraint between the time derivative of its position vector p_{sb} and its spatial angular velocity ω_{sb}

$$\dot{p}_{sb} = r\omega_{sb} \times e_3 = r\hat{\omega}_{sb}e_3, \tag{1}$$

where we introduced the *hat* $\wedge$ operator, which stands for the standard isomorphism between $\mathbb{R}^3$ and $\mathfrak{so}(3)$. Its inverse is denoted by the symbol $\vee$, known as the *vee* map [13].

The kinematics of the orientation of the ball and the top are given in the spatial frame by

$$\dot{R}_{sb} = \hat{\omega}_{sb}R_{sb}, \quad \dot{R}_{st} = \hat{\omega}_{st}R_{st}. \tag{2}$$

Using notation and methods from [13], we express the velocity of the top with respect to the inertial frame V_{st} in terms of the velocity of the ball with respect to the inertial frame V_{sb} and the velocity of the top with respect to the ball V_{bt}

$$V_{st} = V_{sb} + Ad_{g_{sb}}V_{bt} = \begin{bmatrix} v_{sb} + R_{sb}v_{bt} + p_{sb} \times R_{sb}\omega_{bt} \\ \omega_{sb} + R_{sb}\omega_{bt} \end{bmatrix}, \tag{3}$$

where v_{bt} and ω_{bt} are the linear and angular components of V_{bt}. The following calculation shows that the linear velocity of the top with respect to the ball vanishes.

$$\begin{aligned} \hat{V}_{bt} &= \dot{g}_{bt}g_{bt}^{-1} = \frac{\mathrm{d}}{\mathrm{d}t}\left(\begin{bmatrix} R_{bt} & lR_{bt}e_3 \\ 0 & 1 \end{bmatrix}\right)\begin{bmatrix} R_{bt}^\top & -le_3 \\ 0 & 1 \end{bmatrix} \\ &= \begin{bmatrix} \hat{\omega}_{bt}R_{bt} & l\hat{\omega}R_{bt}e_3 \\ 0 & 0 \end{bmatrix}\begin{bmatrix} R_{bt}^\top & -le_3 \\ 0 & 1 \end{bmatrix} = \begin{bmatrix} \hat{\omega}_{bt} & 0 \\ 0 & 0 \end{bmatrix}, \end{aligned} \tag{4}$$

where g_{bt} is the homogeneous transformation of the top with respect to the ball. Substituting (4) into (3) yields

$$V_{st} = \begin{bmatrix} v_{st} \\ \omega_{st} \end{bmatrix} = \begin{bmatrix} v_{sb} + p_{sb} \times R_{sb}\omega_{bt} \\ \omega_{sb} + R_{sb}\omega_{bt} \end{bmatrix}. \tag{5}$$

Now, we compute the time derivative of p_{st}:

$$\begin{aligned} \dot{p}_{st} &= v_{st} + \omega_{st} \times p_{st} \\ &= v_{sb} + p_{sb} \times R_{sb}\omega_{bt} + \omega_{st} \times p_{st} \\ &= \dot{p}_{sb} - \omega_{sb} \times p_{sb} + p_{sb} \times R_{sb}\omega_{bt} + \omega_{sb} \times p_{st} + R_{sb}\omega_{bt} \times p_{st} \\ &= \dot{p}_{sb} + \omega_{st} \times (p_{st} - p_{sb}) \\ &= \dot{p}_{sb} + \omega_{st} \times p_{bt} \\ &= \dot{p}_{sb} + l\omega_{st} \times R_{st}e_3. \end{aligned} \tag{6}$$

Throughout this paper, the dot product of two vectors is denoted by $x \cdot y = x^T y$ for any $x, y \in \mathbb{R}^n$. Unless it is conspicuous from the context, the $n \times n$ identity matrix is denoted by I_n. Simiarly, the $n \times m$ matrix composed of zero elements is denoted by $0_{n\times m}$, and it is written as 0_n if $n = m$. Some properties of the hat map that we freely use in the remainder are as follows

$$\begin{aligned} \hat{x}y &= x \times y = -y \times x = -\hat{y}x, \\ x \cdot \hat{y}z &= y \cdot \hat{z}x = z \cdot \hat{x}y, \\ \hat{x}\hat{y}\hat{z} &= (x \cdot z)\,y - (x \cdot y)\,z, \end{aligned}$$

for any $x, y, z \in \mathbb{R}^3$.

B. Lagrangian

We write the Lagrangian of the ballbot in the spatial frame, that is, as seen by an observer stationary in the inertial frame. Note that it is imperative that the rolling constraint (1) not be inserted into the Lagrangian before its variation is taken. If the variation of the Lagrangian is taken after the substitution of the nonholonomic constraints, this yields the vakonomic equations, which are known to disagree with the dynamics of rigid bodies. Instead, one should take the variation before the imposition of the nonholonomic constraints, leading to the Lagrange-d'Alembert equations, the correct equations of motion [14], [15]. The inertia of the ball and the top expressed in the inertial frame $I_b, I_t \in \mathrm{Sym}^2(Q)$, respectively, are positive-definite symmetric $(0,2)$-tensor fields on Q. Their respective masses are denoted by m_b and m_t.

The kinetic energy of the ball is given by the sum of its rotational and translational kinetic energies, while its potential energy is zero, since its height with respect to the inertial frame remains a constant

$$\begin{aligned} K_b &= \frac{1}{2}\omega_{sb} \cdot I_b\omega_{sb} + \frac{1}{2}m_b\dot{p}_{sb} \cdot \dot{p}_{sb}, \\ V_b &= 0. \end{aligned}$$

The potential energy of the top is given by the height of its center of mass from the horizontal times its mass. The kinetic energy of the top can be written in terms of the rotational velocity of the top and the translational velocity of the ball with respect to the inertial frame by substituting from (6):

$$\begin{aligned}K_t &= \frac{1}{2}\omega_{st}\cdot I_t\omega_{st} + \frac{1}{2}m_t\dot{p}_{st}\cdot\dot{p}_{st}\\ &= \frac{1}{2}\omega_{st}\cdot I_t\omega_{st} + \frac{1}{2}m_t l^2\omega_{st}\cdot\omega_{st} + \frac{1}{2}m_t\dot{p}_{sb}\cdot\dot{p}_{sb} - \frac{1}{2}m_t l^2(\omega_{st}\\ &\quad\cdot R_{st}e_3)^2 + m_t l\dot{p}_{sb}\cdot(\omega_{st}\times R_{st}e_3),\\ V_t &= m_t g l e_3\cdot R_{st}e_3.\end{aligned}$$

Therefore, the Lagrangian is

$$L = K - V = K_t + K_b - V_t \tag{7a}$$

$$\begin{aligned}&= \frac{1}{2}\omega_{st}\cdot I_t\omega_{st} + \frac{1}{2}m_t l^2\omega_{st}\cdot\omega_{st} + \frac{1}{2}\omega_{sb}\cdot I_b\omega_{sb}\\ &\quad + \frac{1}{2}(m_b+m_t)\dot{p}_{sb}\cdot\dot{p}_{sb} - \frac{1}{2}m_t l^2(\omega_{st}\\ &\quad\cdot R_{st}e_3)^2 + m_t l\dot{p}_{sb}\cdot(\omega_{st}\times R_{st}e_3) - m_t g l e_3\cdot R_{st}e_3.\end{aligned} \tag{7b}$$

C. Euler-Lagrange equations

We derive concise and coordinate-invariant equations of motion of the ballbot. By restricting the full dynamics to the x-z plane, we derive the 2D dynamics of the ballbot. This procedure recovers the 2D equations of motion explicitly presented in the literature [4], [5].

We freely make use of the following identities when taking the variation of the Lagrangian (7):

$$\delta R^{-1} = -R^{-1}\delta R R^{-1}, \tag{8a}$$
$$\delta I_t = \delta R_{st}R_{st}^{-1}I_t - I_t\delta R_{st}R_{st}^{-1}, \tag{8b}$$
$$\delta I_b = \delta R_{sb}R_{sb}^{-1}I_b - I_b\delta R_{sb}R_{sb}^{-1}, \tag{8c}$$
$$\delta\hat{\omega}_{st} = \dot{\hat{\eta}}_{st} + \hat{\eta}_{st}\hat{\omega}_{st} - \hat{\omega}_{st}\hat{\eta}_{st}, \tag{8d}$$
$$\delta\hat{\omega}_{sb} = \dot{\hat{\eta}}_{sb} + \hat{\eta}_{sb}\hat{\omega}_{sb} - \hat{\omega}_{sb}\hat{\eta}_{sb}, \tag{8e}$$
$$\delta\dot{p}_{sb} = \frac{\mathrm{d}}{\mathrm{d}t}(\delta p_{sb}). \tag{8f}$$

where we have defined the variation $\hat{\eta}_{st} := \delta R_{st}R_{st}^{-1}$ and similarly for η_{sb}. Computing the variation of the Lagrangian

$$\begin{aligned}\delta L &= \frac{1}{2}(\langle\delta\omega_{st}, I_t\omega_{st}\rangle + \langle\omega_{st},(\delta I_t)\omega_{st} + I_t\delta\omega_{st}\rangle) + m_t l^2\langle\delta\omega_{st},\\ &\quad\omega_{st}\rangle + \frac{1}{2}(\langle\delta\omega_{sb}, I_b\omega_{sb}\rangle + \langle\omega_{sb},(\delta I_b)\omega_{sb}\\ &\quad + I_b\delta\omega_{sb}\rangle) + (m_b+m_t)\langle\delta\dot{p}_{sb},\dot{p}_{sb}\rangle - (\omega_{st}\\ &\quad\cdot R_{st}e_3)m_t l^2(\langle\delta\omega_{st}, R_{st}e_3\rangle + \langle\omega_{st},(\delta R_{st})e_3\rangle)\\ &\quad + m_t l(\langle\delta\dot{p}_{sb},\omega_{st}\times R_{st}e_3\rangle\\ &\qquad + \langle\dot{p}_{sb},\delta\omega_{st}\times R_{st}e_3 + \omega_{st}\times(\delta R_{st})e_3\rangle)\\ &\quad - m_t g l\langle e_3,\delta(R_{st})e_3\rangle\\ &= \langle(I_t + m_t l^2)\omega_{st},\dot{\eta}_{st}\rangle + \langle I_b\omega_{sb},\dot{\eta}_{sb}\rangle\\ &\quad + (m_b+m_t)\langle\dot{p}_{sb},\frac{\mathrm{d}}{\mathrm{d}t}(\delta p_{sb})\rangle - (\omega_{st}\cdot R_{st}e_3)m_t l^2(\langle\dot{\eta}_{st} +\\ &\quad\eta_{st}\times\omega_{st}, R_{st}e_3\rangle + \langle\omega_{st},\eta_{st}\\ &\quad\times R_{st}e_3\rangle) + m_t l\left(\langle\frac{\mathrm{d}}{\mathrm{d}t}(\delta p_{sb}),\omega_{st}\times R_{st}e_3\rangle + \langle\dot{p}_{sb},(\dot{\hat{\eta}}_{st} +\right.\\ &\quad\left.\hat{\eta}_{st}\hat{\omega}_{st})R_{st}e_3\rangle\right) + m_t g l\langle I_t\omega_{st}\times\omega_{st} + e_3\times R_{st}e_3,\eta_{st}\rangle.\end{aligned}$$

Next, we take the variation of the action $S = \int L\,\mathrm{d}t$ using integration by parts with vanishing variations at the endpoints

$$\begin{aligned}\delta S &= \int\delta L\,\mathrm{d}t\\ &= \int -\langle(I_t + m_t l^2)\dot{\omega}_{st} + (\omega_{st}\cdot R_{st}e_3)m_t l^2\omega_{st}\times R_{st}e_3\\ &\quad - m_t l\ddot{p}_{sb}\times R_{st}e_3 + I_t\omega_{st}\times\omega_{st} - m_t g l e_3\times R_{st}e_3,\eta_{st}\rangle\\ &\quad + \langle -I_b\dot{\omega}_{sb},\eta_{sb}\rangle - \langle(m_b+m_t)\frac{\mathrm{d}}{\mathrm{d}t}\dot{p}_{sb} - m_t l(\dot{\omega}_{st}\\ &\quad\times R_{st}e_3 + \omega_{st}\times(\omega_{st}\times R_{st}e_3)),\delta p_{sb}\rangle\,\mathrm{d}t.\end{aligned}$$

Finally, we insert the nonholonomic constraint (1) and its variational form $\delta p_{sb} = r\eta_{sb}\times e_3$

$$\begin{aligned}\delta S &= \int -\langle(I_t + m_t l^2)\dot{\omega}_{st} + (\omega_{st}\\ &\quad\cdot R_{st}e_3)m_t l^2\omega_{st}\times R_{st}e_3 - m_t r l(\dot{\omega}_{sb}\\ &\quad\times e_3)\times R_{st}e_3 + I_t\omega_{st}\times\omega_{st} - m_t g l e_3\times R_{st}e_3,\eta_{st}\rangle\\ &\quad + \langle -I_b\dot{\omega}_{sb} - (m_b+m_t)r^2(\dot{\omega}_{sb}\times e_3)\times e_3 + m_t r l(\dot{\omega}_{st}\\ &\quad\times R_{st}e_3 + \omega_{st}\times(\omega_{st}\times R_{st}e_3))\times e_3,\eta_{sb}\rangle\,\mathrm{d}t.\end{aligned}$$

Keeping accordance with the literature, we assume that the rotation of the ball along the inertial z-axis cannot be actuated and is always a constant during the motion of the ballbot. We consider the scenario where the relative orientation between the ball and the top is actuated as in [5], [7]. In other words, the control input belongs to the subbundle of the cotangent bundle of Q, characterized by the annihilator of the relative angular velocity ω_{tb}: $\tau' \in \{\sigma\in\mathfrak{so}^*(3) : \langle\sigma,\omega_{tb}\rangle = 0\}$, after its identification with $\mathbb{R}^3$. We notice that $\hat{\omega}_{tb} = Ad_{R_{st}^T}(\hat{\omega}_{sb} - \hat{\omega}_{st})$ and using the dual of this mapping, we find the forced Euler-Lagrange equations of motion of the ballbot.

$$M(q)\dot{v} + C(q,v) + G(q) = B(q)\tau', \tag{9}$$

where $q = (R_{st}, R_{sb})$, $v = (\omega_{st},\omega_{sb})$, $\tau'\in\mathbb{R}^3$ and

$$\begin{aligned}&M(q)\\ &= \begin{bmatrix} I_t + m_t l^2(I_3 - R_{st}e_3\otimes e_3^T R_{st}^T) & m_t r l R_{st}\hat{e}_3 R_{st}^T\hat{e}_3^T\\ m_t r l\hat{e}_3 R_{st}\hat{e}_3^T R_{st}^T & I_b - (m_b+m_t)r^2\hat{e}_3^2\end{bmatrix},\\ &C(q,v) = \begin{bmatrix} m_t l^2(\omega_{st}\cdot R_{st}e_3)R_{st}\hat{e}_3 R_{st}^T\omega_{st} + I_t\omega_{st}\times\omega_{st}\\ m_t r l\hat{e}_3\hat{\omega}_{st}^2 R_{st}e_3\end{bmatrix},\\ &G(q) = \begin{bmatrix}-m_t g l\hat{e}_3 R_{st}e_3\\ 0\end{bmatrix}, \qquad B(q) = -\begin{bmatrix} I_3\\ \hat{e}_3^2\end{bmatrix}R_{st}.\end{aligned}$$

These equations are appended by the rolling constraint (1) to yield the Euler-Lagrange equations of motion of the ballbot.

III. Dynamic Properties of the Uncontrolled Ballbot

In this section, we discuss the equilibrium configurations, the repercussions of the rolling constraint regarding LaSalle's invariance principle, and the local eigenstructure of the linearized dynamics.

A. Equilibrium Configurations

When $\tau = 0$, we can determine the equilibria of the ballbot using the equations of motion (9) with the rolling contraint (1). Along with the fact that the inertial z-axis rotation of the ball is assumed to be stationary, the rolling constraints yields $\dot{p}_{sb} = 0 \Longleftrightarrow \omega_{sb} = 0$. Inserting $p_{sb} = \text{constant}$ and $\omega_{sb} = 0$ into the equations of motion (9) along with $\omega_{st} \equiv 0$ yields $e_3 \times R_{st} e_3 = 0$. In other words, the uncontrolled equilibria of the ballbot are given by

$$\begin{aligned} E_{\pm} \ = \{&(p_{sb}, R_{sb}, R_{st}, \dot{p}_{sb}, \omega_{sb}, \omega_{st}) \in TQ : \omega_{sb} = \omega_{st} = 0, \\ &\dot{p}_{sb} = 0,\ p_{sb} = \text{const},\ R_{sb} = \text{const},\ R_{st} e_3 = \pm e_3\}. \end{aligned}$$

Notice that E_+ corresponds to the upward equilibrium point, that is, the top points in the inertial positive z-direction and E_- corresponds to the downward equilibrium point. Due to the rolling constraint and the assumption that the ball does not have an angular velocity along the inertial z-axis, asymptotic stabilization of the translation of the ball is necessary and sufficient for the asymptotic stabilization of its orientation by LaSalle's invariance principle.

B. Linearized Equations of Motion

We are interested in deriving the local dynamics around the upward equilibrium set; that is, the local dynamics in a tubular neighborhood of the set E_+. The derivation of these local equations involves taking the first-order variation of the nonlinear equations of motion (9). We notice that one omits the terms in $C(q,v)$ since they are quadratic in ω_{st}. The terms in the expressions $\delta M(q)\dot{v}$ and $\delta B(q)\tau$ vanish due to the neighborhood in which the linearization is performed. Therefore, in a first approximation, the terms that remain are

$$M(q)|_{R_{st}=I_3} \delta v + \delta G(q)|_{R_{st}=I_3} = B(q)|_{R_{st}=I_3} \delta\tau,$$

which yields the linearized dynamics of the ballbot around the upward equilibrium point

$$M_{\text{lin}} \ddot{\eta} + G_{\text{lin}} \eta = B_{\text{lin}} \delta\tau, \tag{10}$$

where $\eta = (\eta_{st}, \eta_{sb})$ and

$$M_{\text{lin}} = M(I_3, I_3), \quad B_{\text{lin}} = B(I_3, I_3), \quad G_{\text{lin}} = \begin{bmatrix} m_t g l \hat{e}_3^2 & 0_3 \\ 0_3 & 0_3 \end{bmatrix},$$

and the rolling constraint (1) remains unchanged since it is already linear.

The local eigenstructure near the upward equilibrium point can be determined from these linearized dynamics. The eigenvalues of (10) are the roots of $\det\left[\lambda^2 M_{\text{lin}} + G_{\text{lin}}\right] = 0$. Note that there are zero eigenvalues since the last three columns and rows of G_{lin} are zero. These correspond to the ball dynamics. There are yet two more eigenvalues at zero, corresponding to the rotation of the top around the inertial z-axis. The remaining eigenvalues come in positive and negative pairs since the remaining terms in the $(1,1)$ block of G_{lin} yield a negative definite matrix. This implies that the upward equilibrium point of the ballbot is an unstable saddle. Notice that the downward equilibrium point of the ballbot turns out to be a stable equilibrium point and therefore, there exist a heteroclinic connection between these two equilibria, providing a nonlocal characterization of the dynamic flow.

IV. Control Analysis

In this section, we derive two distinct feedback control laws. The first control law is intended to achieve asymptotic stabilization of the orientations of the ball and the top to the identity matrix, while the second one targets the asymptotic stabilization of the orientation of the top to the identity matrix and the translation of the ball to a desired location on the plane. From the linearized equations (10), we confirm that the system is controllable in the quotient $\mathbb{R}^{12}/\text{span}\{e_6, e_{12}\}$ of $\mathbb{R}^{12}$, where we have identified the tangent space $T_{q_0}TQ$ at the upward equilibrium point q_0 with $\mathbb{R}^{12}$. The directions that are excluded to form the quotient vector space correspond exactly to the rotation and the angular velocity of the ball along the inertial z-direction . Indeed, we write the linearized equations (10) in the conventional form

$$\dot{\mathbf{x}} = \mathbf{A}\mathbf{x} + \mathbf{B}\mathbf{u},$$

where $\mathbf{x} = (\eta_{st}, \eta_{sb}, \dot{\eta}_{st}, \dot{\eta}_{sb})$, $\mathbf{u} = \delta\tau$, and the various matrices are given by

$$\mathbf{A} = \begin{bmatrix} 0_3 & 0_3 & I_3 & 0_3 \\ 0_3 & 0_3 & 0_3 & I_3 \\ D_1\hat{e}_3^2 & 0_3 & 0_3 & 0_3 \\ D_2\hat{e}_3^2 & 0_3 & 0_3 & 0_3 \end{bmatrix}, \quad \mathbf{B} = \begin{bmatrix} 0_3 \\ 0_3 \\ D_3 \\ D_4\hat{e}_3^2 \end{bmatrix},$$

where $D_2 > 0$ and $D_1, D_3, D_4 < 0$ are 3×3 diagonal matrices. Due to this form of the state matrix $\mathbf{A}$, it is readily seen that $\text{image}\,(A^n) \subseteq \text{image}\left(\begin{bmatrix} A & A^2 & A^3 \end{bmatrix}\right)$, for $n \geq 4$. Consequently, we can form the controllability matrix from the pair $(\mathbf{A}, \mathbf{B})$ by using only $\mathbf{B}$ and the first three powers of $\mathbf{A}$:

$$\mathscr{C} = \begin{bmatrix} 0 & D_3 & 0 & D_3 D_1 \hat{e}_3^2 \\ 0 & D_4\hat{e}_3^2 & 0 & D_3 D_2 \hat{e}_3^2 \\ D_3 & 0 & D_3 D_1 \hat{e}_3^2 & 0 \\ D_4\hat{e}_3^2 & 0 & D_3 D_2 \hat{e}_3^2 & 0 \end{bmatrix}$$

It is readily verified that $\text{image}\,(\mathscr{C}) \oplus \text{span}\{e_6, e_{12}\} = \mathbb{R}^{12}$. We recognize that the subspace $\text{span}\{e_6, e_{12}\}$ consists of variations of the orientation and the angular velocity of the ball around the inertial z-axis. We denote by the pair $(\tilde{\mathbf{A}}, \tilde{\mathbf{B}})$ the controllable subsystem of $(\mathbf{A}, \mathbf{B})$, whose corresponding state and control input are denoted by $\tilde{\mathbf{x}}$ and $\tilde{\mathbf{u}}$, respectively.

We retain our standing assumption that this motion of the ball is mechanically constrained. Under this assumption, the orientation of the top and the ball are asymptotically stabilized by the control force, τ chosen as follows

$$\begin{aligned} \tau = -\frac{1}{2} K_p \begin{bmatrix} \left(R_{st} - R_{st}^T\right)^{\vee} \\ \left(e_3 e_3^T R_{sb} - R_{sb}^T e_3 e_3^T\right)^{\vee} \end{bmatrix} - K_d \begin{bmatrix} \omega_{st} \\ \left(\hat{\omega}_{sb} e_3 e_3^T + e_3 e_3^T \hat{\omega}_{sb}\right)^{\vee} \end{bmatrix}. \end{aligned} \tag{11}$$

where $K_p, K_d \in \mathbb{R}^{3\times 6}$ both of whose 3×3 blocks are symmetric, positive definite matrices. Indeed, in light of the following calculations

$$
\begin{aligned}
\frac{1}{2}(\delta(R-R^\top))|_{R=I_3} &= \frac{1}{2}\left(R^\top\hat{\eta}+\hat{\eta}R\right)|_{R=I_3}=\hat{\eta},\\
(\delta\hat{\omega})|_{\omega=0} &= \dot{\hat{\eta}},\\
\frac{1}{2}(\delta(e_3e_3^\top R-R^\top e_3e_3^\top))|_{R=I_3} &= \frac{1}{2}\left(\hat{\eta}e_3e_3^\top+e_3e_3^\top\hat{\eta}\right)\\
&= \hat{\eta}-\hat{\eta}_z,\\
(\delta\hat{\omega}e_3e_3^\top+e_3e_3^\top\delta\hat{\omega})|_{\omega=0} &= \dot{\hat{\eta}}-\dot{\hat{\eta}}_z,
\end{aligned}
$$

where $\hat{\eta}_z := \left(\begin{bmatrix}0 & 0 & \eta_z\end{bmatrix}^\top\right)^\wedge$, it can be verified that the variation of the control law (11) corresponds to the conventional state feedback $\tilde{\mathbf{u}} = -\mathbf{K}\tilde{\mathbf{x}}$, which is known to exponentially stabilize the origin of the controllable subsystem [16]. Consequently, the orientation of the ball and the top are locally exponentially stabilized by the control law (11).

It is often the case that we do not care about the final orientation of the ball as long as the orientation of the top and the translation of the ball are asymptotically stabilized to their desired locations. We recall from the previous section III-A that this implies that the orientation of the ball is asymptotically stable, too. This control objective is locally achieved by the following control law

$$
\begin{aligned}
\tau = -\frac{1}{2}K_p\begin{bmatrix}\left(R_{st}-R_{st}^\top\right)^\vee\\ 0\end{bmatrix}\\
-K_d\begin{bmatrix}\omega_{st}\\ \left(\left(\hat{\omega}_{sb}-\hat{\omega}_{sb}^d\right)e_3e_3^\top\right)^\vee+\left(e_3e_3^\top\left(\hat{\omega}_{sb}-\hat{\omega}_{sb}^d\right)\right)^\vee\end{bmatrix},
\end{aligned}
\tag{12}
$$

where $\omega_{sb}^d = e_3\times f_d$, with $f_d = -\frac{k}{r}\begin{bmatrix}x-x_d & y-y_d & 0\end{bmatrix}^\top$, for some $k>0$. The proof of this statement again follows from the calculations leading to the orientation control law (11) in addition to the following arguments regarding the rolling constraint equation (1). We know by the arguments above that $\omega_{sb}\xrightarrow[t\to\infty]{}\omega_{sb}^d$, exponentially fast. Therefore, under the control law (12), we can write the evolution of the translation of the ball as

$$
\begin{bmatrix}\dot{x} & \dot{y} & \dot{z}\end{bmatrix} = -\frac{k}{r}\begin{bmatrix}x-x_d & y-y_d & 0\end{bmatrix}+\begin{bmatrix}\varepsilon_x & \varepsilon_y & 0\end{bmatrix}, \tag{13}
$$

for some $k>0$, where $\varepsilon_x,\varepsilon_y$ are exponentially vanishing perturbations due the exponentially stable nature of ω_{st}. It follows from the vanishing perturbation theory [17] that $R_{st}=I_3$ and $(x_d,y_d,0)$ is a locally exponentially stable equilibrium point of the nonlinear system (9).

V. Numerical Examples

In the subsequent numerical simulations, the inertial properties of the ballbot are taken from [5].

First, simulation results for the uncontrolled ballbot are presented. The initial condition is a small perturbation of the upward equilibrium. More specifically,

$$
\begin{aligned}
R_{st}(0) &= R_{y,\frac{\pi}{360}}R_{x,\frac{\pi}{180}}, \quad \omega_{st}(0)=0,\\
R_{sb}(0) &= I_3, \quad \omega_{sb}(0)=0,\\
p_{sb}(0) &= 0,
\end{aligned}
$$

where the top is perturbed by $\frac{1}{2}^\circ$ along the pitch and 1° along the roll direction from the upward equilibrium. The

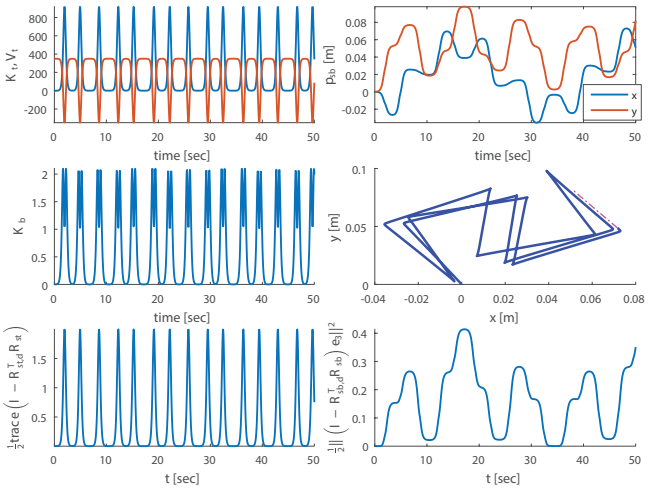

Fig. 2: Unforced response: perturbation from the upward equilibrium

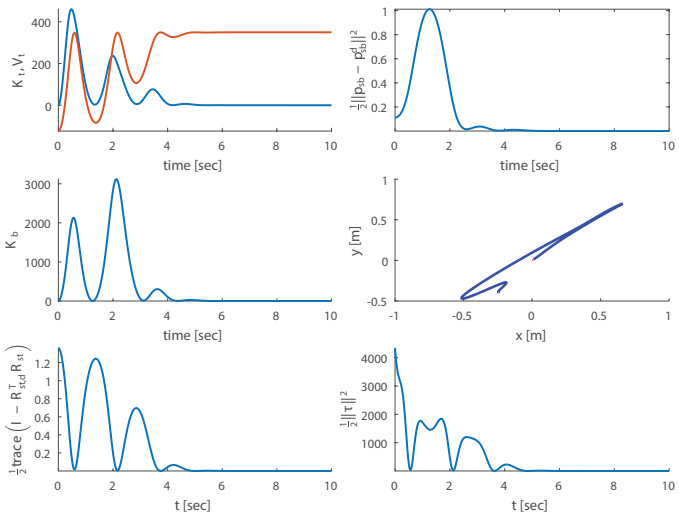

Fig. 3: Controlled response: asymptotic stabilization of the upward equilibrium and desired planar position

corresponding simulation results are shown in Figure 2. The two figures on the top left demonstrates the complex energy transfer between the top and the ball as the ballbot dynamics evolve. On the top right two plots, we observe the unforced translation of the ball performing a chaotic motion around the starting position. The bottom two plots are the amount of rotation the top and the ball undergo from left to right respectively.

Second, simulation results are presented that show the response of the ballbot to a feedback control (12). Even though this controller is derived from the lienarization of the system, simulations indicate that it has a large basin of attraction. Indeed, in this simulation, the initial conditions given by

$$
\begin{aligned}
R_{st}(0) &= R_{z,\frac{2\pi}{3}}R_{y,\frac{3\pi}{4}}R_{x,\frac{\pi}{3}}, \quad \omega_{st}(0)=0,\\
R_{sb}(0) &= I_3, \quad \omega_{sb}(0)=0,\\
p_{sb}(0) &= 0,
\end{aligned}
$$

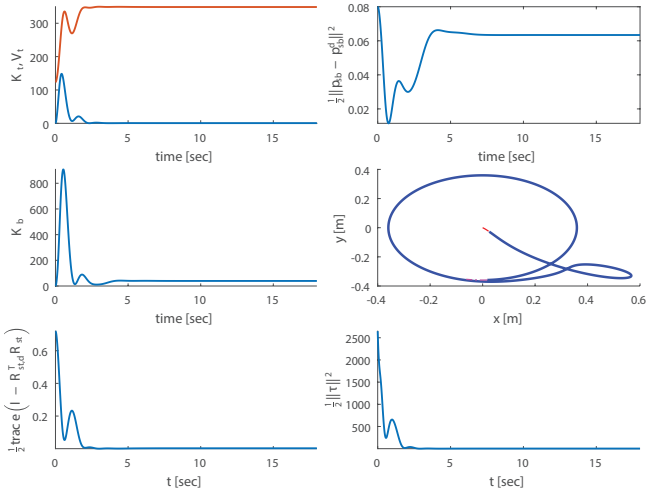

Fig. 4: Controlled response: stabilization of the upward equilibrium and a translational periodic motion

are quite far away from the desired upward equilibrium $R_{st} = I_3$ and the desired planar position $p^d_{sb} = (-0.25, -0.4, 0)$. Figure 3 illustrates the asymptotic stabilization. In the top left two figures, we again see the kinetic and potential energies of the top and the ball. The kinetic energies go to zero since the motion exponentially comes to a stop while the potential energy converges to $m_t \cdot g \cdot l$. In the top right figure, we see the convergence of the translation of the ball to the desired location along with the path the ball takes to get there. In the bottom left figure, we see the orientation of the top converging to identity. Finally on the bottom right plot, we see the total control effort evolution as the stabilization task is carried out.

Finally, we present the trajectory tracking properties of the same feedback control (12) in Figure 4. Starting from the initial conditions

$$\begin{aligned} R_{st}(0) &= R_{y,\frac{\pi}{3}} R_{x,\frac{\pi}{4}}, \quad \omega_{st}(0) = 0, \\ R_{sb}(0) &= I_3, \quad \omega_{sb}(0) = 0, \\ p_{sb}(0) &= 0, \end{aligned}$$

we set the desired translation of the ball to be $(x_d(t), y_d(t)) = 0.4(\cos\frac{t}{2}, -\sin\frac{t}{2})$. In this case, the kinetic energies of the bodies do not vanish and the potential energy of the top settles at a value a bit smaller than $m_t \cdot g \cdot l$. This arises due to a constant orientation error of the top in order to track the desired circular motion of the ball. There is an expected tracking error in the translational motion of the ballbot because the perturbation (13) which exponentially vanishes in the regulation problem, is only bounded in the tracking problem. The necessary control effort can be observed in the bottom left plot.

VI. Conclusion

Euler-Lagrange equations that evolve on $Q = \mathbb{R}^2 \times SO(3) \times SO(3)$ have been derived for the ballbot. We are able to analyze dynamic properties and derive control laws that achieve asymptotic stabilization for a number of purposes thanks to the particularly compact form of these equations of motion.

We emphasize that modeling, analysis and computations can be carried out directly in terms of a geometric coordinate-free framework as illustrated for the ballbot in this paper. This fact facilitates the analysis of the dynamics and control synthesis for complex systems such as the ballbot.

As a future avenue of research, we would like to explore the basin of attraction of suitable controllers developed through the coordinate-free framework by performing a Lyapunov-based analysis. We also intend to further support the developed theory in this paper by performing experiments after designing and implementing a ballbot in our laboratory.

References

[1] H. G. Nguyen, J. Morrell, K. D. Mullens, A. B. Burmeister, S. Miles, N. Farrington, K. M. Thomas, and D. W. Gage, "Segway robotic mobility platform," in *Optics East*. International Society for Optics and Photonics, 2004, pp. 207–220.

[2] T. Lauwers, G. Kantor, and R. Hollis, "One is enough!" in *Proc. Intl. Symp. for Robotics Research*, 2005, pp. 12–15.

[3] T. Lauwers, G. A. Kantor, and R. L. Hollis, "A dynamically stable single-wheeled mobile robot with inverse mouse-ball drive," in *Robotics and Automation, 2006. ICRA 2006. Proceedings 2006 IEEE International Conference on*. IEEE, 2006, pp. 2884–2889.

[4] U. Nagarajan, A. Mampetta, G. A. Kantor, and R. L. Hollis, "State transition, balancing, station keeping, and yaw control for a dynamically stable single spherical wheel mobile robot," in *IEEE International Conference on Robotics and Automation (ICRA), 2009*, May 2009, pp. 998–1003.

[5] U. Nagarajan, G. Kantor, and R. Hollis, "The ballbot: An omnidirectional balancing mobile robot," *The International Journal of Robotics Research*, vol. 33, no. 6, pp. 917–930, 2013.

[6] L. Hertig, D. Schindler, M. Bloesch, C. Remy, and R. Siegwart, "Unified state estimation for a ballbot," in *Robotics and Automation (ICRA), 2013 IEEE International Conference on*, May 2013, pp. 2471–2476.

[7] S. Leutenegger and P. Fankhauser, "Modeling and control of a ballbot," *Bachelor thesis*, 2010.

[8] M. Kumaga and T. Ochiai, "Development of a robot balanced on a ball: Application of passive motion to transport," in *Robotics and Automation, 2009. ICRA '09. IEEE International Conference on*, May 2009, pp. 4106–4111.

[9] U. Nagarajan, G. Kantor, and R. Hollis, "Integrated planning and control for graceful navigation of shape-accelerated underactuated balancing mobile robots," in *IEEE International Conference on Robotics and Automation (ICRA), 2012*, May 2012, pp. 136–141.

[10] U. Nagarajan, B. Kim, and R. Hollis, "Planning in high-dimensional shape space for a single-wheeled balancing mobile robot with arms," in *IEEE International Conference on Robotics and Automation (ICRA), 2012*, May 2012, pp. 130–135.

[11] C.-W. Liao, C.-C. Tsai, Y. Y. Li, and C.-K. Chan, "Dynamic modeling and sliding-mode control of a ball robot with inverse mouse-ball drive," in *SICE Annual Conference, 2008*, Aug 2008, pp. 2951–2955.

[12] A. Inal, O. Morgul, and U. Saranli, "A 3D dynamic model of a spherical wheeled self-balancing robot," in *Intelligent Robots and Systems (IROS), 2012 IEEE/RSJ International Conference on*, Oct 2012, pp. 5381–5386.

[13] R. M. Murray, S. S. Sastry, and L. Zexiang, *A Mathematical Introduction to Robotic Manipulation*, 1st ed. Boca Raton, FL, USA: CRC Press, Inc., 1994.

[14] A. D. Lewis and R. M. Murray, "Variational principles for constrained systems: theory and experiment," *International Journal of Non-Linear Mechanics*, vol. 30, no. 6, pp. 793–815, 1995.

[15] J. Baillieul, A. Bloch, P. Crouch, and J. Marsden, *Nonholonomic Mechanics and Control*, ser. Interdisciplinary Applied Mathematics. Springer New York, 2008.

[16] C.-T. Chen, *Linear system theory and design*. Oxford University Press, Inc., 1995.

[17] H. Khalil, *Nonlinear Systems*. Prentice Hall, 2002.